Journal of Orthopaedic Surgery and Research

RESEARCH

Open Access

Mogroside V enhances bone marrow mesenchymal stem cells osteogenesis under hyperglycemic conditions through upregulating miR-10b-5p and PI3K/Akt signaling

Dongni Lan[1,2†], Kongmei Li[1,2†], Zhimao Ye[1,2], Yicai Luo[1,2], Cuiping Li[1,2] and Hao Li[1,2*]

Abstract

Background Mogroside V (MV) is a triterpene glucoside that reportedly exhibits an array of antitumor, anti-inflammatory, hypolipidemic, and hypoglycemic properties. In prior studies, our group determined that MV was able to readily enhance osteogenic bone marrow mesenchymal stem cells (BMSCs) differentiation under high-glucose conditions through mechanisms potentially associated with miR-10b-5p and PI3K/Akt signaling activity. The precise molecular basis for these effects, however, remains to be fully elucidated.

Objective This study aims to explore the potential mechanisms by which MV regulates the osteogenic differentiation of BMSCs under hyperglycemic conditions.

Methods Femoral and tibial BMSCs were isolated from control and diabetic C57BL/6J mice. qRT-PCR was used to quantify miR-10b-5p levels. Putative miR-10b-5p target genes were predicted through bioinformatics assays and validated in a luciferase reporter assay system. miR-10b-5p expression was inhibited with an antagomiR-10b-5p construct, while PI3K/Akt pathway signaling was inhibited with LY294002. Western blotting was used to detect PI3K/Akt pathway and target gene protein levels, while Alizarin red staining was used to detect calcium nodule deposition by BMSCs.

Results miR-10b-5p upregulation was noted in BMSCs exposed to hyperglycemic conditions. HOXD10 was identified as a cell differentiation-related miR-10b-5p target gene in bioinformatics analyses, and the targeting relationship between the two was confirmed in a luciferase reporter assay. MV treatment elicited significantly higher levels of miR-10b-5p expression, PI3K phosphorylation, and calcium deposition, while antagomiR-10b-5p or LY294002 treatment reversed these changes, and the opposite trends were observed with respect to HOXD10 protein levels.

†Dongni Lan and Kongmei Li contributed equally to this work as co-first authors.

*Correspondence:
Hao Li
sherrylee2011@126.com

Full list of author information is available at the end of the article

Conclusion MV favors BMSCs osteogenic differentiation under high-glucose conditions through the upregulation of miR-10b-5p and the activation of PI3K/Akt signaling.

Keywords Mogroside V, Diabetes, Bone marrow mesenchymal stem cells, Osteogenic differentiation, miR-10b-5p, PI3K/Akt

Introduction

The prevalance of diabetes has risen markedly in recent years. These patients are exposed to conditions of persistent hyperglycemia that place their quality of life and overall health at serious risk, such that diabetes remains a major public health concern throughout the globe [1, 2]. Diabetes mellitus can contribute to an elevated risk of developing periodontitis, further impairing glycemic control and exacerbating related complications thereof [3]. Osteoporosis and impaired bone healing are often observed in diabetic individuals when assessing the alveolar bone in edentulous areas [4], making implant restoration more challenging. Chronic hyperglycemia can significantly impair BMSCs osteogenic differentiation, interfering with normal wound healing after teeth have been extracted [5]. In addition to impairing BMSCs proliferation [6], hyperglycemia can trigger premature apoptosis [7], induce ferroptosis [8], and favor lipogenic differentiation [9]. No reliable therapies have been established that are suitable for the management of diabetic alveolar bone defects in clinical settings. As a result, there remains a pressing need to devise new approaches to managing the impaired healing of these defects in individuals with diabetes.

Mogroside V (MV) is a natural bioactive compound that has recently been reported to exhibit an array of functions, including pro-proliferative, antioxidant, and anti-inflammatory properties [10–12]. A prior report published by our team demonstrated that MV can significantly enhance the osteogenic differentiation of BMSCs stimulated by high-glucose conditions. Altered miRNA expression profiles observed in this context highlighted the potential relevance of exploring the mechanistic importance of miR-10b-5p and the PI3K/Akt axis in this cytological context [13].

MiRNAs are pivotal regulators of skeletal homeostasis, with emerging evidence highlighting their roles in modulating bone metabolism and degenerative conditions such as osteoarthritis [14]. Earlier reports have demonstrated the involvement of miR-10b-5p in diabetes regulation. For instance, hepatic expression of this miRNA has been demonstrated to be significantly elevated as compared to normal control animals [15]. Functionally, miR-10b-5p may enhance pancreatic β-cell function and can control glucose homeostasis [16]. There is also evidence that miR-10b-5p exhibits anti-inflammatory functionality [17]. Signaling via the PI3K/Akt axis is central to the osteogenic differentiation of mesenchymal stem cells, with PI3K/Akt pathway activation inducting the osteoblastic differentiation of human BMSCs [18].

In this study, BMSCs were isolated from diabetic mice and exposed to high-glucose culture conditions in the presence or absence of MV. A series of experiments were integrated with the results of preliminary small molecule high pathway sequencing results to investigate the effects of MV on miR-10b-5p levels and PI3K/Akt pathway signaling under hyperglycemic conditions to modulate BMSCs functionality. The findings provide an evidence-based reference for the application of MV as a tool to help remediate the poor alveolar bone defect healing observed in diabetic patients.

Materials and methods

Animals and diabetes models

C57BL/6J mice (males, 3 weeks old; $n = 15$) from the Laboratory of Experimental Animals at Guangxi Medical University (Nanning, China) were used for this study. These mice had free access to soft food. After being allowed 1 week to acclimatize, they were assigned at random to normal (N, $n = 5$) and diabetes (DM, $n = 10$) groups. The Animal Ethics Committee of Guangxi Medical University approved this study (#2020-0004), which was performed in accordance with all relevant guidelines.

Mice in DM group received high-fat diets (20% carbohydrate, 20% protein, and 60% fat) for 3 weeks. The following week (week 5 of the study), they were fasted for 12 h and intraperitoneally injected with 1% 1% streptozotocin (90 mg/kg; Solarbio, China). Seventy-two hours later, the fasting blood glucose (FBG) level was determined using blood collected from the tail vein, repeating these measurements on days 7, 14, and 21 after STZ injection. FBG ≥ 11.1 mmol/L was the threshold used to confirm successful DM modeling. The animals in N group received control diets with intraperitoneal administration of an equivalent amount of citric acid-sodium citrate buffer.

Cell culture

BMSCs were harvested from the femurs and tibiae of N and DM mice as in a prior study [19]. BMSCs from DM mode mice (DM-BMSCs) were grown with high-glucose DMEM (H-DMEM; Gibco, USA), whereas N-BMSCs were cultured with low-glucose DMEM

(L-DMEM; Gibco). The media in both groups contained 15% fetal bovine serum (Gibco) and 1% penicillin/streptomycin (Solarbio, China) and were changed every third day. Cells in all groups were cultured in a 5% CO_2 37 °C incubator with controlled humidity (ThermoFisher Scientific, Japan). An inverted microscope (Olympus, Japan) was used to monitor the growth and morphology of these cells on a daily basis.

DM-BMSCs were separated into DM and DM + MV groups, while BMSCs from mice in the N group were considered N-BMSCs. These BMSCs were added to 6-well plates (1×10^5/well) until 70% confluent, after which cells in the N group were treated with low-glucose osteogenic induction medium, whereas those in DM and DM + MV groups were treated with high-glucose osteogenic induction medium, with the cells in the latter group also having MV 6.25×10^{-3} g/L added to their medium.

Flow cytometry

Characteristic BMSCs surface markers were analyzed via flow cytometry. Briefly, BMSCs (1×10^7 cells/mL in PBS with 0.1% BSA [Biofroxx, Germany]) were stained with antibodies specific for CD73, CD90, CD45, and CD11b (Solarbio, China) for 30 min at 4 °C away from light. They were then assessed via flow cytometry (BD Celesta, USA).

qRT-PCR

TRIzol was used to extract total RNA from BMSCs as directed by the manufacturer, after which cDNA was prepared with a primer sequence RT-PCR kit (Thermo Scientific, USA). TBGreen® premixed ExTaq™II (Tli RNaseH Plus) (TaKaRa, Japan) was then used to perform qRT-PCR analyses, with U6 as a normalization control using primers listed in Table 1. Relative expression was determined with the $2^{-\Delta\Delta Ct}$ method.

Predictive target gene identification

The overlap between the miRDB, TargetScan, and miRTarBase databases was used for the prediction of miRNA target genes.

Luciferase reporter assay

Wild-type (WT) or mutant (Mut) HOXD10 sequence variants were synthesized by GeneCham and then introduced into the GV272 reporter construct (GeneChem). HEK-293T cells were then co-transfected with WT-HOXD10 or Mut-HOXD10 reporters together with miR-10b-5p or a negative control construct and a Renilla luciferase reporter vector. Following a 48 h incubation, a dual-luciferase reporter assay system (UE) was utilized to quantify luciferase activity.

Table 1 Primer sequences

Gene	Direction	Sequence(5′-3′)
miR-10b-5p	F	GCGTACCCTGTAGAACCGAATTTGTG
U6	F	GGAACGATACAGAGAAGATTAGC
	R	TGGAACGCTTCACGAATTTGCG

Cell treatments

Osteogenic induction was achieved by treating BMSCs with group-specific formulations. Specifically, cells in the N group were treated with low-glucose osteogenic induction medium, whereas cells in DM and DM + MV groups were treated with high-glucose osteogenic induction medium, with MV supplementation (6.25×10^{-3} g/L) in the latter of these two groups. Cells in DM + MV + antagomiR NC and DM + MV + antagomiR-10b-5p groups, cells were treated under conditions identical to those for DM + MV group with the addition of 50 nmol/L antagomiR NC of antagomiR-10b-5p (Bioengineering Biologicals, China), respectively. Cells in DM + MV + LY294002 group were treated under conditions identical to those for DM + MV group with the addition of 10 μmol/L LY294002 (MedChemExpress, Inc., USA). Cells in DM + MV + antagomiR-10b-5p + LY294002 group were treated with high-glucose osteogenic induction medium containing 6.25×10^{-3} g/L MV, 50 nmol/L antagomiR-10b-5p, and 10 μmol/L LY294002. Following induction for 7 days, cells were analyzed byqRT-PCRand Western blotting, while Alizarin red staining was performed on day 14.

Western blotting

Western blotting was utilized to assess PI3K/Akt pathway and HOXD10 protein levels. Briefly, cells from each treatment group were lysed in separate tubes in 50 μL of RIPA lysis buffer (Shanghai Yamei Biologicals, China), followed by sonication for 5 min to extract proteins. Total protein levels in the supernatant fraction were then quantified with a BCA assay (Epilepsy Biomedical Technology Co., Ltd., China). After separating total protein by 12.5% SDS-PAGE, they were transferred to PVDF membranes (Millipore, USA) that were probed overnight with antibodies specific for β-actin (1:10,000) (Wuhan Three Eagles Biotechnology Co., Ltd., China), PI3K (1:1,750), p-PI3K (1:1,250), and HOXD10 (1:500) at 4 °C. Following three rinses using TBST (Solarbio, China), samples were probed with secondary antibodies for 1 h based on dilutions recommended by the manufacturer, washed three more times (10 min/wash), treated with developer solution for 90 s in the dark, and then scanned with an imaging instrument.

Alizarin red staining

BMSCs were fixed using 4% paraformaldehyde (Sigma-Aldrich, USA) for 15 min, after which they were stained with ARS solution (Solarbio, China). Osteogenic nodules were stained orange-red in color, and were imaged via microscopy. The ARS solution was then removed by adding cetylpyridinium chloride solution (Macklin Biochemical Co., Ltd., Shanghai, China). Absorbance at 562 nm was analyzed with a plate reader to compare calcium deposition in the different groups based on relative absorbance levels.

Statistical analyses

Western immunoblots were analyzed with ImageJ. Data are presented as means ± standard deviation (*SD*), and were compared with one-way ANOVA with SNK-q multiple comparisons tests GraphPad Prism 9.5 (USA). All analyses were performed three or more times, with $P < 0.05$ being defined as significant.

Results

Morphologic and phenotypic analyses of BMSCs and validation of differential miR-10b-5p expression

Both the N-BMSCs and DM-BMSCs in this study exhibited spindle-shaped morphology when examined on day 7 of culture (Fig. 1a, b). Flow cytometry analyses revealed that both N-BMSCs and DM-BMSCs showed CD73 and CD90 positivity but were negative for CD45 and CD11b (Fig. 1c, d), validating successful BMSC purification. In PCR andqRT-PCRanalyses, elevated miR-10b-5p expression was found in N and DM + MV groups in comparison with DM group (Fig. 1e).

Prediction of miR-10b-5p target genes

Next, miR-10b-5p sequences were identified with the miRWalk website, after which putative targets of this miRNA were identified with the TargetScan, miRTarBase, and miRDB databases. Based on the overlap between predictions from these three databases, 8 putative target genes were selected (Fig. 2; Table 2). A review of published studies demonstrated a link between HOXD10 and cellular differentiation, prompting further studies of HOXD10 as a target for additional validation.

Luciferase-based confirmation of interactions between miR-10b-5p and HOXD10

Established WT-HOXD10, Mut-HOXD10, and miR-10b-5p fragment sequences are presented in Fig. 3a. Co-transfection of WT-HOXD10 and miR-10b-5p mimics, significant reductions in luciferase activity were noted relative to that associated with the miRNA-NC, while luciferase activity was not

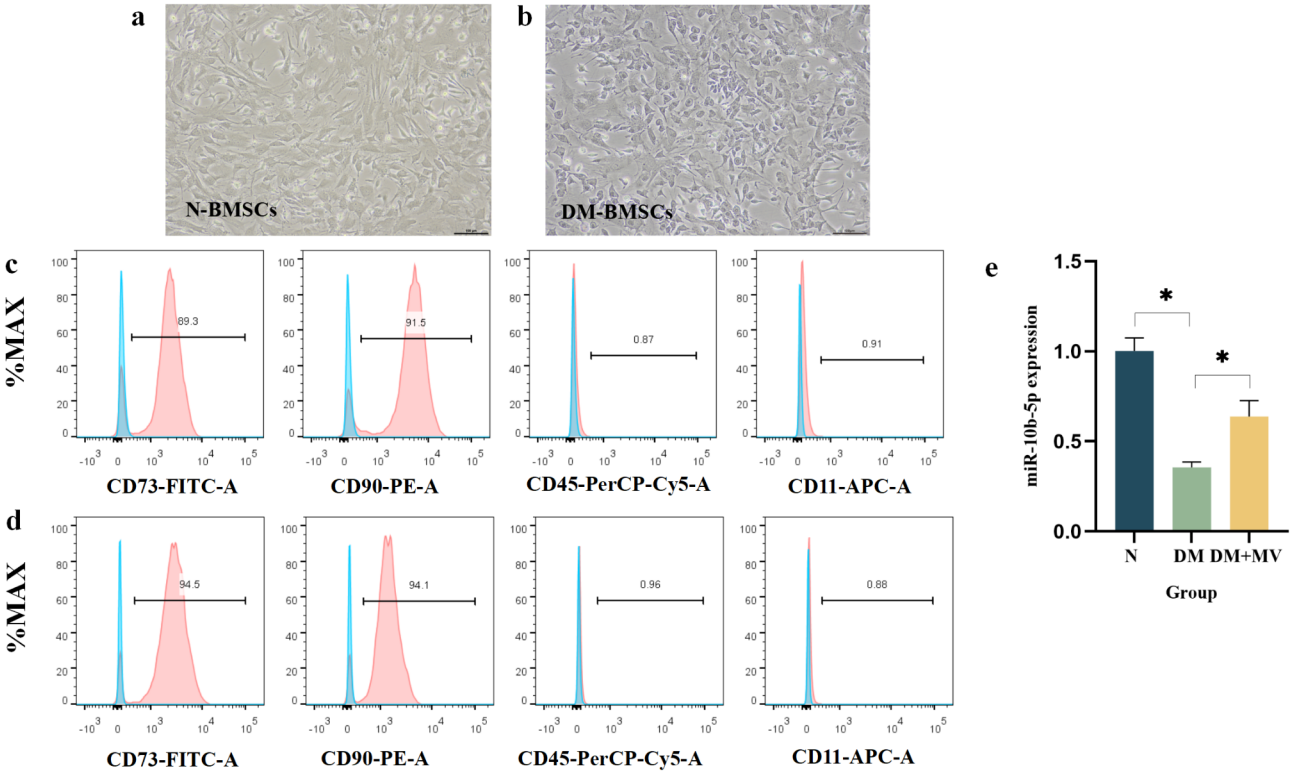

Fig. 1 (**a**) BMSCs in normal control group (Scale bar = 100 μm). (**b**) BMSCs in diabetic group (Scale bar = 100 μm). N-BMSCs (**c**) and DM-BMSCs (**d**) surface markers were identified by flow cytometry. (**e**) Relative miR-10b-5p expression in each group

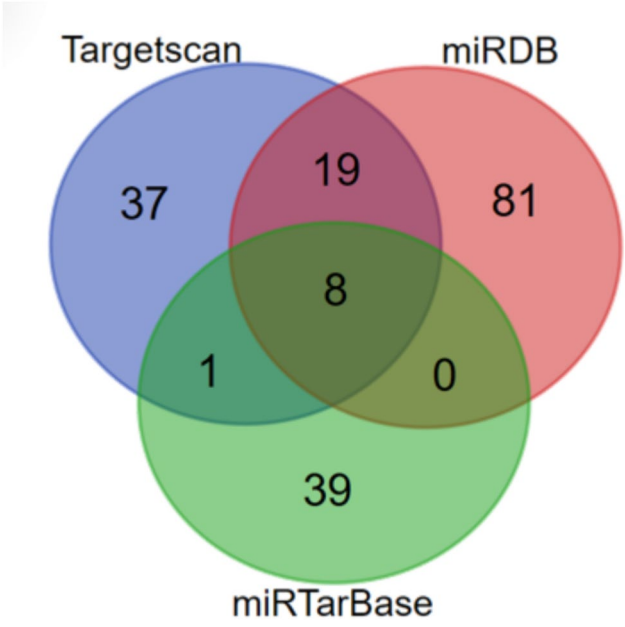

Fig. 2 Intersecting miR-10b-5p target genes

Table 2 Predicted miR-10b-5p target genes

miRNA	Predicted Relevant Target Genes
miR-10b-5p	ELAVL3, EPHA5, GABRB2, HOXB3, HOXD10, MAPKBP1, NR4A3, RHPN2, TIAM1

significantly affected when Mut-HOXD10 was used instead (Fig. 3b).

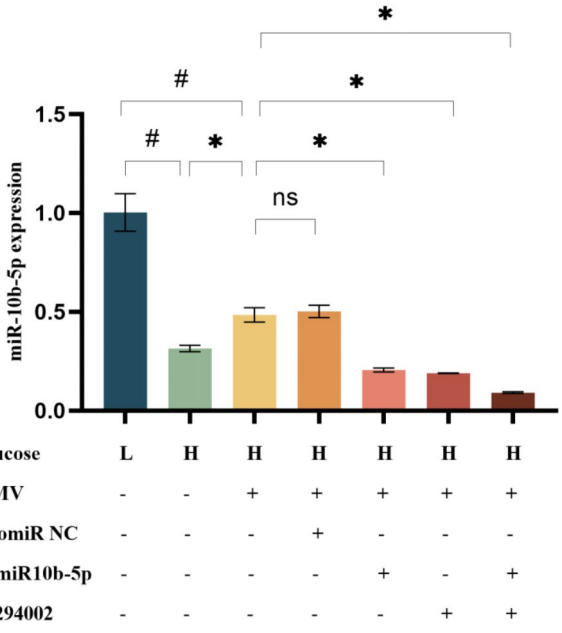

Fig. 4 Relative miR-10b-5p expression in individual groups. Note: $^{\#}P < 0.05$ vs. N group; $^{*}P < 0.05$ vs. DM + MV group; ns, not significant

miR-10b-5p detection

A significant reduction in miR-10b-5p levels was noted in DM group compared with the N group ($P < 0.05$), while an increase in levels were seen in DM + MV group in comparison with DM + MV group ($P < 0.05$), while these levels were lower in DM + MV + antagomiR-10b-5p, DM + MV + LY294002, and DM + MV + antagomiR-10b-5p + LY294002 groups relative to DM + MV group ($P < 0.05$) (Fig. 4).

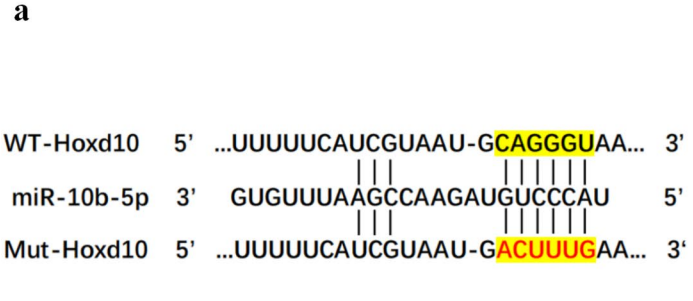

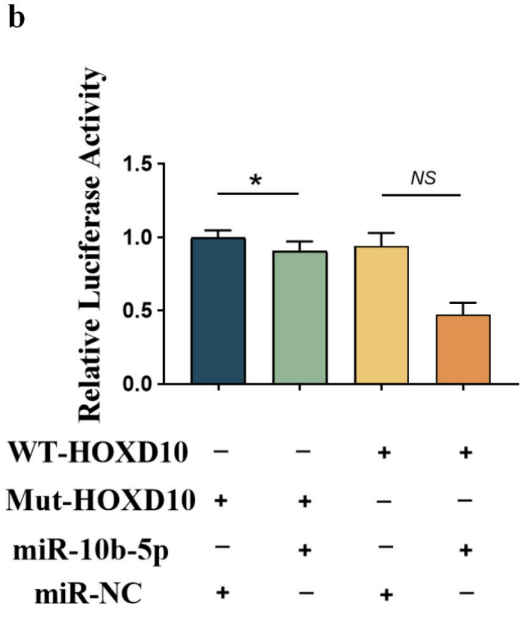

Fig. 3 (**a**) WT- and Mut-HOXD10 3'-UTR sequences for miR-10B-5p. (**b**) WT- and Mut-HOXD10 3'-UTR luciferase reporter constructs were co-transfected into 293T cells along with miR-10b-5p mimics or miRNA negative control constructs. Luciferase activity was quantified at 48 h post-transfection

HOXD10 and PI3K/Akt signaling-related protein analyses

Western blotting analyses revealed significantly higher protein levels of HOXD10 in the DM group compared with N group ($P < 0.05$) (Fig. 5a) while reduced levels were noted in DM + MV group in comparison with DM group ($P < 0.05$) and increased levels in DM + MV + antagomiR-10b-5p, DM + MV + LY294002, and DM + MV + antagomiR-10b-5p + LY294002 groups ($P < 0.05$). A significant reduction in PI3K phosphorylation was noted in DM group compared with N group ($P < 0.05$) (Fig. 5b), while these levels were elevated in DM + MV group compared with DM group ($P < 0.05$). A decrease in such phosphorylation was also noted in DM + MV + antagomiR-10b-5p, DM + MV + LY294002, and DM + MV + antagomiR-10b-5p + LY294002 groups ($P < 0.05$).

Alizarin red staining results

In ARS and quantitative analyses, higher levels of calcium nodule deposition were noted in DM groups compared with N group ($P < 0.05$) (Fig. 6), while significantly increased calcium deposition was apparent in DM + MV group relative to DM group ($P < 0.05$). However, such calcium deposition was inhibited in DM + MV + antagomiR-10b-5p, DM + MV + LY294002, and DM + MV + antagomiR-10b-5p + LY294002 groups ($P < 0.05$) (Fig. 7).

Discussion

BMSCs undergo appropriate osteogenic differentiation to preserve bone homeostasis as a component of the normal dynamics of bone metabolism [20]. In patients with diabetes mellitus, persistent hyperglycemia can severely impair BMSCs osteogenesis, thereby disrupting the normal balance of bone metabolism [21]. Here, exposure to high-glucose conditions was confirmed to inhibit BMSCs osteogenesis, whereas this trend was reversed by MV exposure, in line with the present results.

A previous miRNA-seq analysis conducted by our group comparing BMSCs from control, diabetic, and MV-treated diabetic mice identified miR-10b-5p as the only miRNA that was differentially expressed when comparing each of these pairs of groups [13]. There have also been some prior reports linking miR-10b-5p to osteogenesis and glucose homeostasis. In male mice, for instance, miR-10b-5p knockout is associated with the onset of diabetes, whereas glucose homeostasis can be improved by injection of an miR-10b-5p mimic [22, 23]. The silencing of miR-10b-5p can also suppress osteogenic factor expression and promote apoptotic death in human BMSCs [24]. In some reports, a significant reduction in miR-10b-5p levels was noted in patients who had recently suffered osteoporotic fractures or were affected by postmenopausal

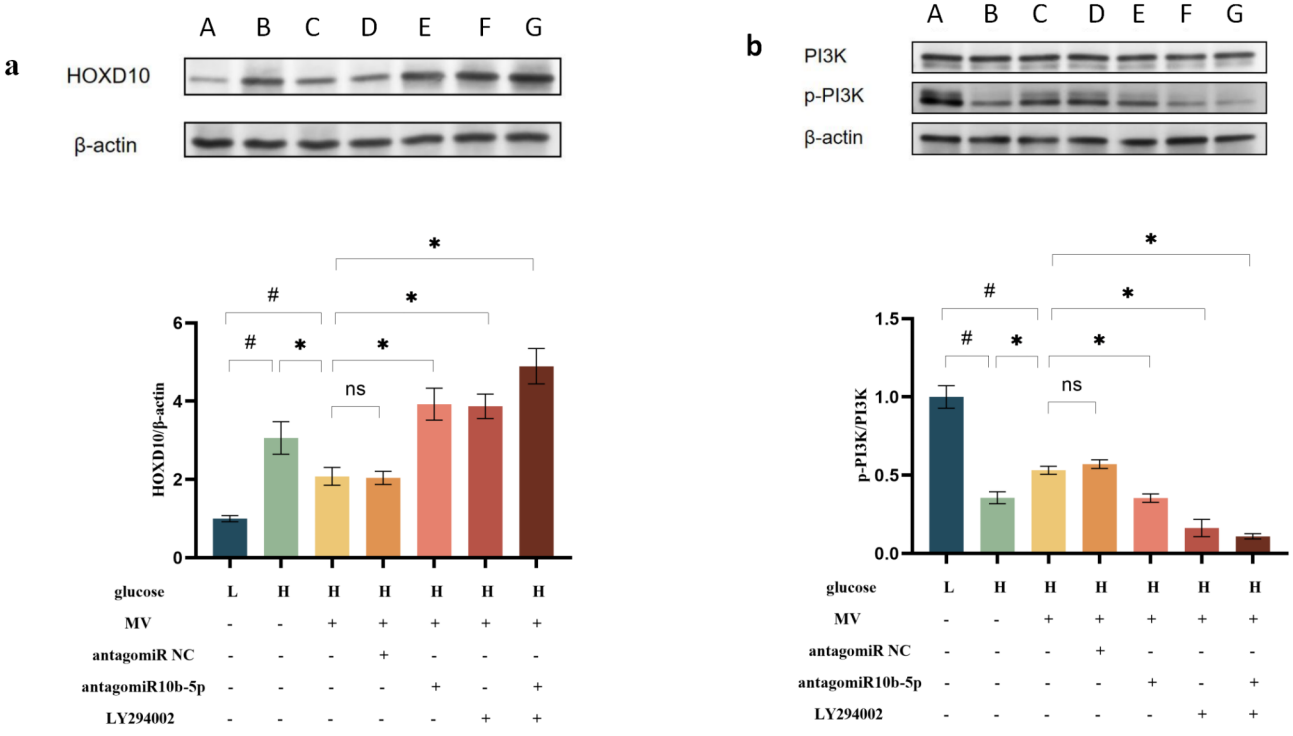

Fig. 5 HOXD10 and PI3K, p-PI3K protein levels in individual experimental groups. Note: In Fig. 5**a**, **b** and A-G respectively correspond to the N (A), DM (B), DM + MV (C), DM + MV + antagomir NC (D), DM + MV + antagomiR-10b-5p (E), DM + MV + LY294002 (F), and DM + MV + antagomiR-10b-5p + LY294002 (G). #$P < 0.05$ vs. N; *$P < 0.05$ vs. DM + MV; ns, not significant

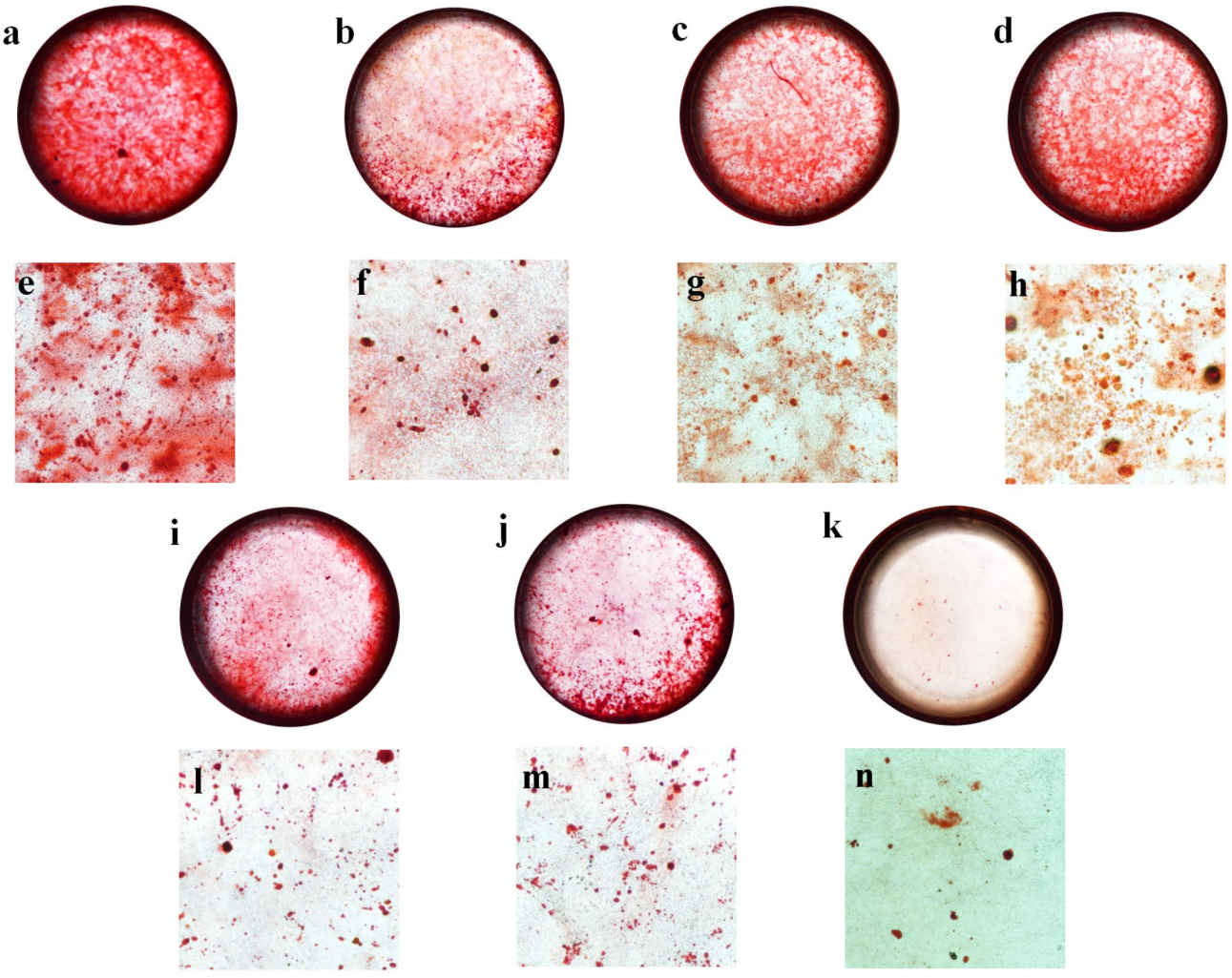

Fig. 6 Alizarin red staining results. Note: In Fig. 6, **a-n** show individual groups, including the N group (**a**, **e**), DM group (**b**, **f**), DM + MV group (**c**, **g**), DM + MV + antagomir NC group (**d**, **h**), DM + MV + antagomiR-10b-5p group (**i**, **l**), DM + MD + LY294002 group (**j**, **m**), and DM + MV + antagomiR-10b-5p + LY294002 group (**k**, **n**). In e, f, g, h, l, m, and n 40-fold magnification is shown

osteoporosis [25, 26]. Here, the ability of MV to promote BMSC osteogenic differentiation while exposed to high glucose levels was confirmed to be mediated by increases in miR-10b-5p expression.

Signaling through the PI3K/Akt axis is central to the control of insulin homeostasis and can also shape the osteogenic differentiation of BMSCs [27]. Stimulation of the PI3K/Akt axis can induce the osteoblastic transformation of human BMSCs, thereby driving osteogenesis [28]. PI3K/Akt signaling activity can limit oxidative stress, foster improved survival, and enhance the osteogenic differentiation of BMSCs exposed to high glucose levels [29]. Here, high glucose levels were found to inhibit PI3K activation of BMSCs, whereas MV was able to reverse this inhibitor effect. LY294002, the first synthesized PI3K inhibitor, is now widely utilized in studies of the PI3K/Akt axis [30]. Treatment with LY294002 was herein found to suppress MV-induced PI3K/Akt phosphorylation in BMSCs under high-close conditions, while simultaneously reversing the osteogenic differentiation of these MV-treated cells. The inhibition of miR-10b-5p in these cells was also sufficient to suppress MV-induced PI3K/Akt phosphorylation. Based on these findings, it appears that MV can promote BMSCs osteogenesis under hyperglycemic conditions by activating the miR-10b-5p/PI3K/Akt signaling axis. In one prior report, MV was demonstrated to attenuate LPS-induced inflammation in RAW264.7 cells by inhibiting PI3K/Akt pathway signaling [31]. This is in opposition with the observed effects of MV on PI3K/Akt signaling in the present study, potentially owing to differences in the regulation of miR-10b-5p. In one recent report, miR-10b-5p was shown to induce PI3K/Akt signaling activity in glioma cells, thus promoting their glycometabolic reprogramming [32]. There is also evidence

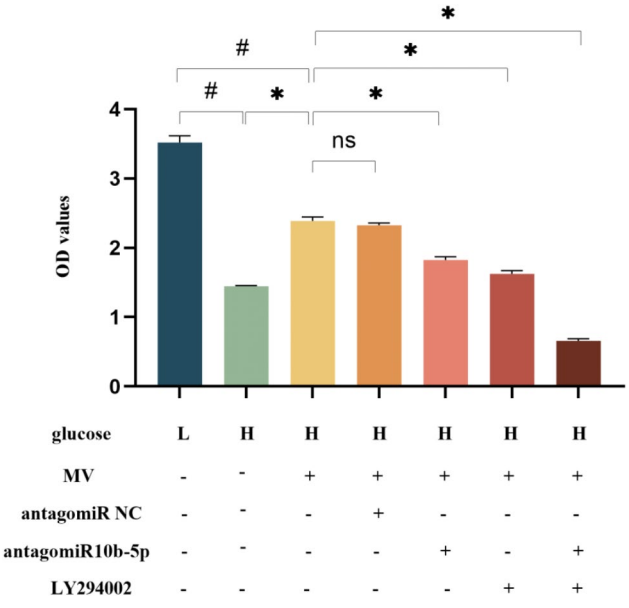

Fig. 7 Quantitative analysis of alizarin red OD values for each group. Note: $^{\#}P < 0.05$ compared to N group; $^{*}P < 0.05$ compared to DM + MV group; ns no statistical difference

that miR-10b-5p can positively regulate the PI3K/Akt axis in HASMCs to suppress stretch-induced apoptotic death [33]. These links between miR-10b-5p and PI3K/Akt activity align with the current findings. Notably, miR-10b-5p was downregulated in cells treated with LY294002, suggesting that signaling activity downstream of PI3K/Akt may feed back to control the expression of miR-10b-5p.

HOXD10 has been repeatedly demonstrated to be a direct target of miR-10b-5p [34, 35], in line with the present results. Members of the HOX gene family are core regulators of developmental processes including organ formation and cellular differentiation in the context of embryogenesis [36]. HOXD10 is an abdominal-B homeobox family transcription factor with a sequence-specific HOX DNA-binding domain [36]. HOXD10 plays a role in chondrogenic differentiation processes in induced pluripotent stem cells from humans [37], and prolonged HOXD10 expression can reportedly impair endothelial cell migration initiated by growth factors such as basic fibroblast growth factor and vascular endothelial growth factor [38]. Additional investigations are required to fully clarify the relationship between HOXD10 and impaired BMSC osteogenesis under conditions of high-glucose exposure.

Conclusion

In summary, the present analyses demonstrated the ability of MV to promote BMSCs osteogenesis under hyperglycemic conditions through processes dependent on miR-10b-5p upregulation. These effects were associated with HOXD10 downregulation and enhanced PI3K/Akt signaling activity. Given these promising results, MV administration at appropriate dose levels may be capable of protecting against diabetes-induced alveolar bone loss. However, this study has several limitations. First, this study lacks in vivo experimental validation, such as diabetic mouse bone defect models. Second, miR-10b-5p mimics were not employed to investigate the effects of miR-10b-5p overexpression on HOXD10, the PI3K/Akt pathway, and BMSC osteogenesis. Furthermore, the expression of osteogenesis-related factors, including Runx2, OPN, and OCN, in BMSCs was not examined following the inhibition of miR-10b-5p and HOXD10. Therefore, future research will specifically address the aforementioned limitations to further elucidate the osteogenic effects and underlying mechanisms of MVs.

Acknowledgements
The authors would like to acknowledge all the personnel from Guangxi Key Laboratory of Oral and Maxillofacial Restoration and Reconstruction, Guangxi Medical University, for their technical support.

Author contributions
DL and KL analyzed the data and wrote the manuscript. HL designed the research and reviewed the manuscript. DL, KL, ZY, YL and CL contributed to data collation and analysis. All authors reviewed the manuscript.

Funding
This work was supported by the National Natural Science Foundation of China (No.82060195) and Joint Project on Regional High-Incidence Diseases Research of Guangxi Natural Science Foundation (No.2023GXNSFAA026264).

Data availability
No datasets were generated or analysed during the current study.

Declarations

Competing interests
The authors declare no competing interests.

Author details
[1]Department of Prosthodontics, College & Affiliated Hospital of Stomatology, Guangxi Medical University, Nanning 530021, Guangxi, China
[2]Guangxi Key Laboratory of Oral and Maxillofacial Restoration and Reconstruction, Guangxi Medical University, Nanning 530021, Guangxi, China

Received: 30 December 2024 / Accepted: 4 March 2025
Published online: 14 March 2025

References

1. Bloomgarden ZT. Diabetes epidemiology: analysis of trends over time. J Diabetes. 2022;14:790–1.
2. Ward ZJ, Yeh JM, Reddy CL, Gomber A, Ross C, Rittiphairoj T, et al. Estimating the total incidence of type 1 diabetes in children and adolescents aged 0–19 years from 1990 to 2050: a global simulation-based analysis. Lancet Diabetes Endocrinol. 2022;10:848–58.
3. Genco RJ, Borgnakke WS. Diabetes as a potential risk for periodontitis: association studies. Periodontol 2000. 2020;83:40–5.

4. Li G, Prior JC, Leslie WD, Thabane L, Papaioannou A, Josse RG, et al. Frailty and risk of fractures in patients with type 2 diabetes. Diabetes Care. 2019;42:507–13.
5. Yang S, Li Y, Liu C, Wu Y, Wan Z, Shen D. Pathogenesis and treatment of wound healing in patients with diabetes after tooth extraction. Front Endocrinol. 2022;13:949535.
6. Li X, Zhan J, Hou Y, Hou Y, Chen S, Luo D, et al. Coenzyme Q10 regulation of apoptosis and oxidative stress in H_2O_2 induced BMSC death by modulating the Nrf-2/NQO-1 signaling pathway and its application in a model of spinal cord injury. Oxidative Med Cell Longev. 2019;2019:1–15.
7. Song L, Liu M, Ono N, Bringhurst FR, Kronenberg HM, Guo J. Loss of wnt/β-catenin signaling causes cell fate shift of preosteoblasts from osteoblasts to adipocytes. J Bone Miner Res. 2012;27:2344–58.
8. Xu C-Y, Xu C, Xu Y-N, Du S-Q, Dai Z-H, Jin S-Q, et al. Poliumoside protects against type 2 diabetes-related osteoporosis by suppressing ferroptosis via activation of the Nrf2/GPX4 pathway. Phytomedicine. 2024;125:155342.
9. Ambrosi TH, Scialdone A, Graja A, Gohlke S, Jank A-M, Bocian C, et al. Adipocyte accumulation in the bone marrow during obesity and aging impairs stem cell-based hematopoietic and bone regeneration. Cell Stem Cell. 2017;20:771–e7846.
10. Shen J, Shen D, Tang Q, Li Z, Jin X, Li C. Mogroside V exerts anti-inflammatory effects on fine particulate matter-induced inflammation in porcine alveolar macrophages. Toxicol in Vitro. 2022;80:105326.
11. Pan C, Chen J, Chen Y, Lu Y, Liang X, Xiong B, et al. Mogroside V ameliorates the oxidative stress-induced meiotic defects in porcine oocytes in vitro. Reprod Toxicol. 2022;111:148–57.
12. Mo Q, Fu H, Zhao D, Zhang J, Wang C, Wang D, et al. Protective effects of Mogroside V on oxidative stress induced by H2O2 in skin fibroblasts. Drug Des Devel Ther. 2021;15:4901–9.
13. Luo Y, Ye Z, Li C, Hong L, Li H, Mogroside V. Promotes osteogenic differentiation of bone marrow mesenchymal stem cells from diabetic mice by altering MicroRNA profiles. Comb Chem High Throughput Screen. 2025;28:998–1010.
14. Oliviero A, Della Porta G, Peretti GM, Maffulli N. MicroRNA in osteoarthritis: physiopathology, diagnosis and therapeutic challenge. Br Med Bull. 2019;130:137–47.
15. Li Z, Zhao H, Chu S, Liu X, Qu X, Li J, et al. miR-124-3p promotes BMSC osteogenesis via suppressing the GSK-3β/β-catenin signaling pathway in diabetic osteoporosis rats. Vitro CellDevBiol-Animal. 2020;56:723–34.
16. Luo M, Zhao Z, Yi J. Osteogenesis of bone marrow mesenchymal stem cell in hyperglycemia. Front Endocrinol. 2023;14:1150068.
17. Hashimoto N, Tanaka T. Role of MiRNAs in the pathogenesis and susceptibility of diabetes mellitus. J Hum Genet. 2017;62:141–50.
18. Wang X, Qian J, Meng Y, Wang P, Cheng R, Zhou G, et al. Salidroside alleviates severe acute pancreatitis-triggered pancreatic injury and inflammation by regulating miR-217-5p/YAF2 axis. Int Immunopharmacol. 2022;111:109123.
19. Ma Z, Liao J, Zhao C, Cai D. Effects of the 1, 4-dihydropyridine L-type calcium channel blocker benidipine on bone marrow stromal cells. Cell Tissue Res. 2015;361:467–76.
20. Li C, Qiu M, Chang L, Qi J, Zhang L, Ryffel B, et al. The osteoprotective role of USP26 in coordinating bone formation and resorption. Cell Death Differ. 2022;29:1123–36.
21. Murray CE, Coleman CM. Impact of diabetes mellitus on bone health. Int J Mol Sci. 2019;20:4873.
22. Singh R, Ha SE, Wei L, Jin B, Zogg H, Poudrier SM, et al. miR-10b-5p rescues diabetes and gastrointestinal dysmotility. Gastroenterology. 2021;160:1662–e167818.
23. Zogg H, Singh R, Ha SE, Wang Z, Jin B, Ha M, et al. miR-10b-5p rescues leaky gut linked with gastrointestinal dysmotility and diabetes. United Eur Gastroenterol J. 2023;11:750–66.
24. Wu Z, Shi M, Zhao X, Wu G, Zheng H, Cui Y, et al. LINC00963 represses osteogenic differentiation of hBMSCs via the miR-10b-5p/RAP2A/AKT Axis. Int J Sports Med. 2024;45:856–66.
25. Wang R, Lu A, Liu W, Yue J, Sun Q, Chen J, et al. Searching for valuable differentially expressed MiRNAs in postmenopausal osteoporosis by RNA sequencing. J Obstet Gynaecol Res. 2020;46:1183–92.
26. Weilner S, Skalicky S, Salzer B, Keider V, Wagner M, Hildner F, et al. Differentially circulating MiRNAs after recent osteoporotic fractures can influence osteogenic differentiation. Bone. 2015;79:43–51.
27. Chen Y, Hu Y, Yang L, Zhou J, Tang Y, Zheng L, et al. Runx2 alleviates high glucose-suppressed osteogenic differentiation via PI3K/AKT/GSK3β/β-catenin pathway. Cell Biol Int. 2017;41:822–32.
28. Fu S, Yan M, Fan Q, Xu J. Salidroside promotes osteoblast proliferation and differentiation via the activation of AMPK to inhibit bone resorption of knee osteoarthritis mice. Tissue Cell. 2022;79:101917.
29. Li Y, Wang X. Chrysin attenuates high glucose-induced BMSC dysfunction via the activation of the PI3K/AKT/Nrf2 signaling pathway. Drug Des Devel Ther. 2022;16:165–82.
30. Sabbah DA, Hajjo R, Bardaweel SK, Zhong HA. Phosphatidylinositol 3-kinase (PI3K) inhibitors: a recent update on inhibitor design and clinical trials (2016–2020). Expert Opin Ther Pat. 2021;31:877–92.
31. Zhou Y, Hu Z, Ye F, Guo T, Luo Y, Zhou W, et al. Mogroside V exerts anti-inflammatory effect via MAPK-NF-κB/AP-1 and AMPK-PI3K/Akt/mTOR pathways in ulcerative colitis. J Funct Foods. 2021;87:104807.
32. Li S, Mao L, Song L, Xia X, Wang Z, Cheng Y, et al. Extracellular vesicles derived from glioma stem cells affect glycometabolic reprogramming of glioma cells through the miR-10b-5p/PTEN/PI3K/Akt pathway. Stem Cell Rev Rep. 2024;20:779–96.
33. Quan R, Liang W, Li H, Ning Q, Shang D. Silencing of miR-10b-5p alleviates the mechanical stretch-induced proliferation of HASMCs. Tissue Cell. 2022;74:101700.
34. Xiao H, Li H, Yu G, Xiao W, Hu J, Tang K, et al. MicroRNA-10b promotes migration and invasion through KLF4 and HOXD10 in human bladder cancer. Oncol Rep. 2014;31:1832–8.
35. Ruan Z, Li Y, He R, Li X. Inhibition of microRNA-10b-5p up-regulates HOXD10 to attenuate Alzheimer's disease in rats via the Rho/ROCK signalling pathway. J Drug Target. 2021;29:531–40.
36. Xu Y, Wang S, Tang C, Chen W. Upregulation of long non-coding RNA HIF 1α-anti-sense 1 induced by transforming growth factor-β-mediated targeting of Sirtuin 1 promotes osteoblastic differentiation of human bone marrow stromal cells. Mol Med Rep. 2015;12:7233–8.
37. Stelcer E, Kulcenty K, Rucinski M, Jopek K, Richter M, Trzeciak T, et al. The role of MicroRNAs in early chondrogenesis of human induced pluripotent stem cells (hiPSCs). Int J Mol Sci. 2019;20:4371.
38. Myers C, Charboneau A, Cheung I, Hanks D, Boudreau N. Sustained expression of homeobox D10 inhibits angiogenesis. Am J Pathol. 2002;161:2099.

Publisher's note